Growth of Calcite Single Crystals Underneath Monolayers of 5,11,17,23-Tetra-*t*-butyl-25,26,27,28-tetrakis(carboxymethoxy)calix[4]arene

Dirk Volkmer* and Marc Fricke

Bielefeld, Fakultät für Chemie der Universität

Dedicated to Professor Bernt Krebs on the Occasion of his 65th Birthday

Abstract. The amphiphilic 5,11,17,23-tetra-*t*-butyl-25,26,27,28-tetrakis(carboxymethoxy)calix[4]arene (**1**) forms stable monolayers at the air-water interface which serve as template to induce growth of $CaCO_3$ (calcite) single crystals. The nucleation density and the preferred orientation(s) of calcite single crystals depend on the surface pressure applied to the monolayer. Models of the pressure-dependant aggregation of amphiphiles at the air-water interface are derived from the crystal structures of the novel Ca coordination compounds $[(Ca(C_{52}H_{60}O_{12}))_2Ca(H_2O)_2(CH_3OH)_3Ca(H_2O)_2(CH_3OH)_2]\cdot 12CH_3OH\cdot 4H_2O$ (**2**) and $[Ca(C_{52}H_{60}O_{12})Ca(H_2O)_{2.5}(MeOH)_{0.5}]\cdot 7H_2O\cdot CH_3OH$ (**3**). Structural data are analyzed in terms of supramolecular packing arrangements and Ca coordination motifs of the constituting amphiphilic macrocycles.

Keywords: Calix[4]arenes; Monolayers; Crystal engineering; Calcite; Biomineralization

Wachstum von Calciteinkristallen unter Monoschichten aus 5,11,17,23-Tetra-*t*-butyl-25,26,27,28-tetrakis(carboxymethoxy)calix[4]aren

Inhaltsübersicht. Das amphiphile 5,11,17,23-Tetra-*t*-butyl-25,26,27,28-tetrakis(carboxymethoxy)calix[4]aren (**1**) bildet an der Wasser-Luft-Grenzfläche stabile Monoschichten, die als Templat für ein gerichtetes Wachstum von $CaCO_3$ (Calcit) Einkristallen dienen. Die Keimdichte und die Vorzugsorientierung(en) der Calciteinkristalle sind abhängig vom Oberflächendruck in der Monoschicht. Modelle für die druckabhängige Aggregation der Amphiphile in der Wasser-Luft-Grenzschicht werden aus Kristallstrukturen der neuartigen Ca-Koordinationsverbindungen $[(Ca(C_{52}H_{60}O_{12}))_2Ca(H_2O)_2(CH_3OH)_3Ca(H_2O)_2(CH_3OH)_2]\cdot 12CH_3OH\cdot 4H_2O$ (**2**) und $[Ca(C_{52}H_{60}O_{12})Ca(H_2O)_{2.5}(MeOH)_{0.5}]\cdot 7H_2O\cdot CH_3OH$ (**3**) abgeleitet. Die Strukturdaten werden im Hinblick auf supramolekulare Packungs- und Ca-Koordinationsmotive der am Aufbau beteiligten amphiphilen Makrozyklen analysiert.

Introduction

Crystallization of inorganic solids at self-organized surfaces is an important process in biomineralization and crystal engineering [1, 2]. Nucleation and growth steps taking place at the interface are often specific and result in a particular crystal morphology or polymorph. In recent years Langmuir monolayers [3] and self-assembled monolayers (SAMs) [4] have been employed as 2D crystallization templates which induce epitaxial growth of highly oriented calcium carbonate crystals, the most abundant biomineral in nature. Physical parameters such as interfacial electrostatics, [2, 4, 5] hydrogen bonding [3, 5] and interfacial molecular recognition events including geometrical lattice matching [2, 3] and stereochemical complementarity [6] were discussed as crucial factors in this context. In order to mimic structural aspects of the interactions between acidic proteins and biogenic calcite in calcified tissues (i. e. mollusk shells) we employ oligoacids based on amphiphilic calix[*n*]arene moieties as biologically inspired supramolecular templates for epitaxial crystal growth [7].

Employing macrocylic amphiphiles we would like to address the rather fundamental question concerning the putative structure of crystal nucleation sites in calcified tissues. Investigations on the amino acid composition of different natural proteins associated with biomineralization reveal sequence motifs which are particularly rich in aspartic acid and glutamic acid residues, respectively [8]. Unfortunately, none of the acidic proteins extracted from calcified tissues have yet been grown into single crystals suitable for X-ray crystallographic investigations and thus three-dimensional structures are currently not available. However, a representative structural model of a mineral/peptide interface architecture may be derived from the iron storage protein (ferritin) which is regarded as an archetypal biological model for the formation of a nanocrystalline mineral phase within a confined space [9]. Here, the ferritin L-chain subunit bears

* Dr. D. Volkmer
Faculty of Chemistry (AC1)
University of Bielefeld
D-33501 Bielefeld (Germany)
P.O. Box 100 131
Telephone: (+49) 521-106 6142
Fax: (+49) 521-106 6003
E-mail: dirk.volkmer@uni-bielefeld.de

four suitably aligned glutamic acid residues that are necessary for mineral formation. Artificial organic molecules can be designed such as to mimic the confined arrangement of acidic residues in natural proteins. Macrocyclic calix[*n*]arenes such as **1** are especially suited for this purpose since they are synthetically readily available. These molecules form confined arrays of co-aligned carboxylic acid groups, the number and relative positions of which show systematic structural variations depending on the size of the macrocyclic backbone.

Here we present the synthesis and X-ray structure analysis of two novel Ca coordination compounds of the amphiphilic ligand 5,11,17,23-tetra-*t*-butyl-25,26,27,28-tetrakis (carboxymethoxy)calix[4]arene (**1**), namely the compounds $[(Ca(C_{52}H_{60}O_{12}))_2Ca(H_2O)_2(CH_3OH)_3Ca(H_2O)_2(CH_3OH)_2]\cdot 12CH_3OH\cdot 4H_2O$ (**2**) and $[Ca(C_{52}H_{60}O_{12})Ca(H_2O)_{2.5}(MeOH)_{0.5}]\cdot 7H_2O\cdot CH_3OH$ (**3**). Monolayers of **1** are spread on an aqueous subphase containing Ca ions and the Langmuir isotherms recorded are analyzed in terms of monolayer stability, aggregation behaviour, and average area/molecule. Models of the putative packing arrangements of calix[4]arene molecules at the air-water interface and possible Ca coordination motifs are derived from crystal data of **2** and **3**.

Results and Discussion

X-ray crystallographic investigations

Although there are quite a few crystal structures of *t*-butylcalix[4]arene derivatives described in literature, a single crystal X-ray structure analysis of a metal complex of the carboxylic acid derivative has not been reported so far. In a previous study [7] we have presented the X-ray structures of 5,11,17,23-tetrakis-(1,1,3,3-tetramethylbutyl)-25,26,27,28-tetra(carboxymethoxy)calix[4]arene ($C_{68}H_{96}O_{12}\cdot 4.75CH_3OH\cdot 0.25H_2O$, **5**) and its corresponding calcium complex $[Ca(C_{68}H_{92}O_{12}Ca)(DMSO)_2(H_2O)]\cdot 2.5DMSO$ (**6**). In this paper we present the X-ray structural data of two Ca complexes of 5,11,17,23-tetra-*t*-butyl-25,26,27,28-tetrakis(carboxymethoxy)calix[4]arene (**1**).

Crystal structure of ***2****.*

Single crystals of the compound $[(Ca(C_{52}H_{60}O_{12}))_2Ca(H_2O)_2(CH_3OH)_3Ca(H_2O)_2(CH_3OH)_2]\cdot 12CH_3OH\cdot 4H_2O$ ($C_{242}H_{408}Ca_8O_{98}$, **2**) were obtained from methanol solution containing 5 vol.% of water. Slow evaporation of the solvent at room temperature leads to formation of colorless (highly fragile) crystals of **2**. Single crystals suitable for X-ray crystallographic investigations were hard to obtain, mainly due to the rapid loss of solvent molecules (within seconds) upon exposing the crystals to air. Consequently the structure refinement converged to a relatively high final R value. The crystal structure of **2** in fact shows that a host of solvent molecules are occluded in the crystal lattice. Most of the atomic positions of the lattice solvent molecules had to be refined with a site occupancy factor below 1.0 which confirms our observation of the rapid aging of the crystals. Furthermore, a fraction of the Ca ions (Ca(4A,B) including their coordinated ligands) are placed at two slightly different crystallographic positions which excluded the possibility of a fully anisotropic refinement).

The X-ray structure analysis shows that **2** consists of an octacalcium coordination compound. The asymmetric unit contains four Ca ions, two of which are strongly sequestered by a calix[4]arene ligand **1**. The unit cell thus contains one formula unit of the complex. The coordination of a single Ca ion to **1** leads to formation of the structurally rigid $[Ca(C_{52}H_{60}O_{12})]^{2-}$ moiety which in turn serves as bridging unit in compound **2**. Two $[Ca(C_{52}H_{60}O_{12})]^{2-}$ moieties are coordinated to four Ca ions in a μ_4-bridging mode, while at the same time two of them act as capping ligand in a μ_2-bridging mode (Fig. 1). The four Ca ions Ca(3), Ca(4A), Ca(3)*, and Ca(4A)* span a plane and the distance of Ca(2) (Ca(1), respectively) at normal direction towards this plane amounts to 3.81 Å (1.45 Å).

The coordination environments of Ca(1) and Ca(2) each consist of eight oxygen donors provided by the calix[4]arene ligand **1**. The square planes spanned by the phenolic and the carboxylate oxygen donors of Ca(1), (Ca(2), respectively), are rotated by 33.3° (29.9°) against each other. The

Table 1 X-Ray crystallographic data for compounds **2** and **3**

Compound	**2**	**3**
Empirical formula	$C_{242}H_{408}Ca_8O_{98}$	$C_{53.5}H_{85}Ca_2O_{23}$
Formula weight	5206.39 g · mol^{-1}	1176.38 g · mol^{-1}
Crystal system	triclinic	orthorhombic
Space group	$P\bar{1}$ (no. 2)	*Pbcn* (no. 60)
Unit cell dimensions	a = 16.526(3) Å b = 21.936(4) Å c = 23.029(5) Å α = 99.36(3)° β = 99.04(3)° γ = 110.13(3)°	a = 49.75(1) Å b = 13.252(3) Å c = 20.068(4) Å
Cell volume	7527(3) Å^3	13231(5) Å^3
Formula units per cell	1	8
Calculated density	1.149 g · cm^{-3}	1.181 g · cm^{-3}
Diffractometer type	SMART 1K (Bruker AXS)	
Temperature	183(2) K	
Radiation (wavelength)	Mo-K$_\alpha$ (0.71073 Å)	
Scan type	ω-scan	
2θ range for data collection	3.18 − 55.74°	6.06 − 52.04°
Index ranges	$0 \le h \le 21$ $-26 \le k \le 25$ $-30 \le l \le 29$	$0 \le h \le 61$ $0 \le k \le 16$ $0 \le l \le 24$
Reflections collected	79513	68146
Independent reflections	31060 [R_{int} = 0.0957]	12527 [R_{int} = 0.0896]
Data / restraints / parameters	31060 / 0 / 1575	12527 / 0 / 733
Structure solution	SHELXS-97	
Refinement Program	SHELXL-97	
Goodness-of-fit	1.561	1.027
Final R indices [I > 2σ(I)]	R_1 = 0.1535, wR_2 = 0.4093	R_1 = 0.1003, wR_2[a)] = 0.2823
R indices (all data)	R_1 = 0.2279, wR_2 = 0.4548	R_1 = 0.1252, wR_2[a)] = 0.3015
Largest peak and hole	1.350 and −1.003 e Å^{-3}	0.966 and −0.677 e Å^{-3}

[a)] $w = 1/[\sigma^2(F_o^2)+(0.1571\cdot P)2+44.09\cdot P]$ with $P = (F_o^2 + 2\cdot F_c^2)/3$

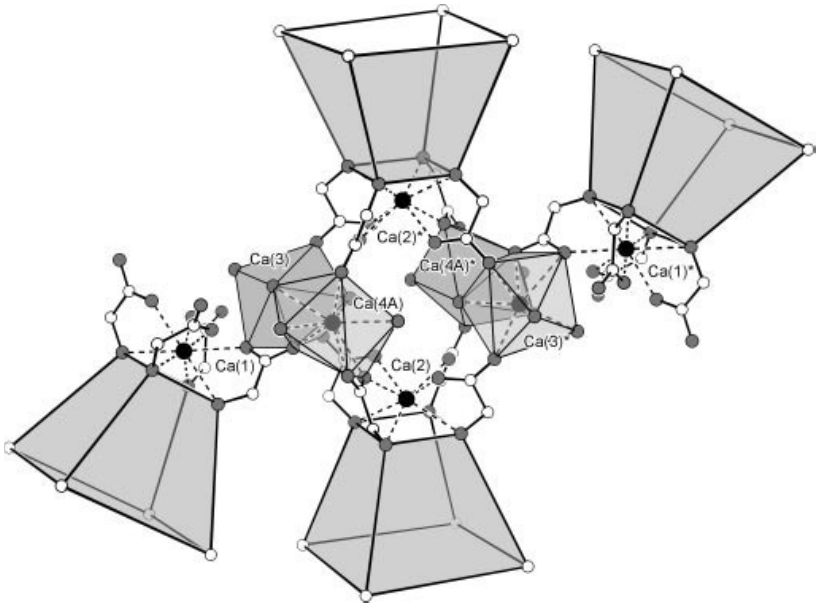

Fig. 1 Simplified representation of the coordination scheme of **2** (coordination polyhedrons are displayed for interconnecting Ca ions only). Selected Ca···Ca non-bonding distances:

Ca(1)···Ca(3): 4.67(7), Ca(1)···Ca(4A): 6.21(6), Ca(3)···Ca(4A): 3.65(7), Ca(2)···Ca(3): 5.91(13), Ca(2)···Ca(4A): 5.44(8), Ca(3)···Ca(4A)*: 7.11(6), Ca(3)···Ca(3)*: 8.99(4) Å.

coordination, therefore, is best described as an intermediate form between a square antiprism and a cube.

The coordination environment of Ca(3) (Ca(4A), respectively) also consists of eight oxygen donors, four of which stem from different calix[4]arene ligands while the other ones belong to coordinated methanol or water ligands. Ca(3) and Ca(4A) form a triply bridged, dinuclear unit with a short Ca···Ca distance of 3.65(7) Å (Fig. 2).

The calix[4]arene molecules adapt a highly symmetrical cone-conformation where the hydrophobic para-*t*-butyl substituents are placed at stereochemically equivalent positions. The pseudo C_{4v} symmetry axis of the μ_4-bridging ligand is tilted by 25° against the plane normal of the *ab* crystal plane while the corresponding tilt angle of the μ_2-bridging calix[4]arene amounts to 18°.

Compound **2** forms a lamellar structure where the hydrophilic constituents (carboxylate residues, Ca ions, crystal methanol and water solvate) and the hydrophobic residues segregate into different layers. This supramolecular packing arrangement is reminiscent of the bilayer structural motif of membrane forming biogenic lipids and likewise amphiphilic molecules [10]. The bilayers run parallel to the crystallographic *ab*-plane and layer stacking follows the *c*-direction (Fig. 3). The average surface area occupied by a single calix[4]arene molecule in the *ab*-plane of the crystal structure of **2** amounts to 1.70 nm^2. This value is considerably higher than the average molecular surface area as determined from the Langmuir isotherms of **1** on an aqueous subphase (see the following section). A closer examination of the crystal structure of **2** indeed shows that the packing arrangement of calix[4]arene residues is interspersed with solvate molecules which leads to holes in the layer structure. The pack-

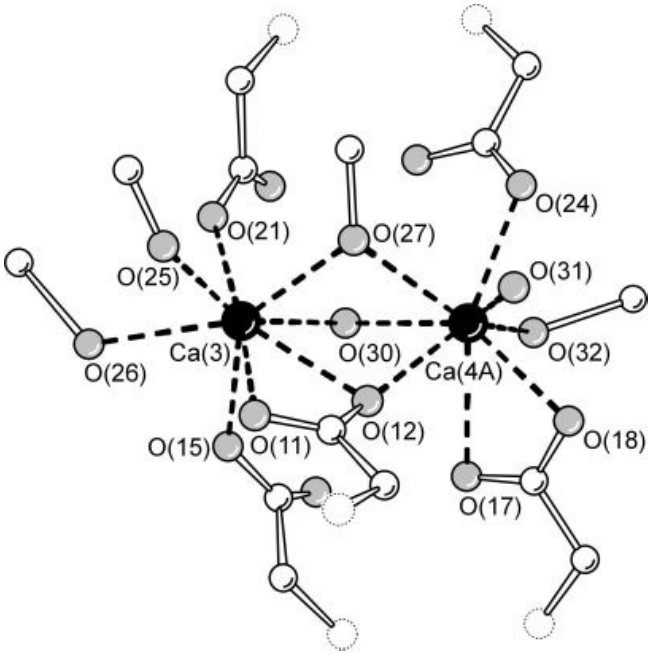

Fig. 2 Ball-and-stick model of the dinuclear Ca centers in the crystal structure of **2**.
(The carboxylate groups shown here are part of different calix[4]arene ligands (**1**), most atoms of which are omitted for clarity). Selected Ca−O bond lengths:

Ca(3)−O(11): 2.62(4), Ca(3)−O(12): 2.55(3), Ca(3)−O(15): 2.33(4), Ca(3)−O(21): 2.29(3), Ca(3)−O(25): 2.40(3), Ca(3)−O(26): 2.52(5), Ca(3)−O(27): 2.53(3), Ca(3)−O(30): 2.43(1), Ca(4A)−O(12): 2.34(6), Ca(4A)−O(17): 2.67(5), Ca(4A)−O(18): 2.26(2), Ca(4A)−O(24): 2.41(7), Ca(4A)−O(27): 2.72(3), Ca(4A)−O(30): 2.47(3), Ca(4A)−O(31): 2.42(2), Ca(4A)−O(32): 2.46(1) Å.

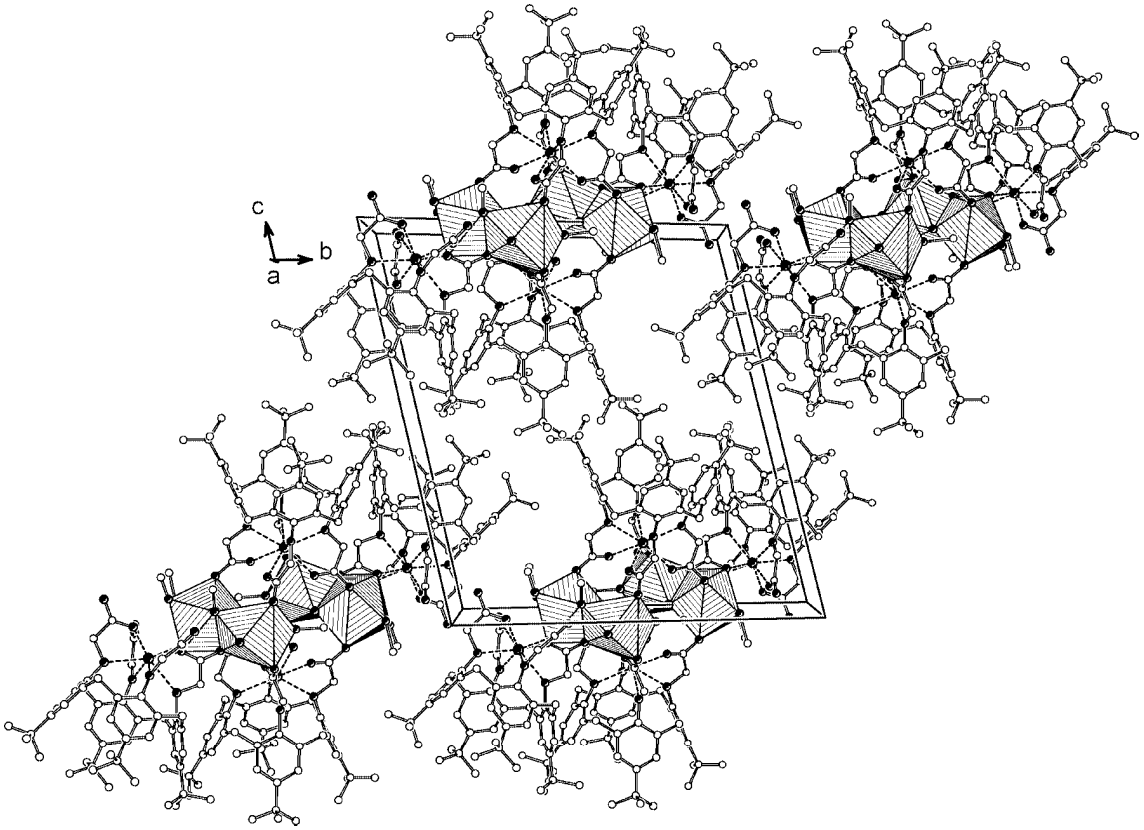

Fig. 3 Ball-and-stick model of the supramolecular packing arrangement of **2** in the crystal lattice. (Hydrogen atoms and non-coordinated solvent molecules are omitted for clarity. Coordination polyhedrons are displayed for interconnecting Ca ions only.)

ing of calix[4]arene ligands in the *ab*-plane of **2** may therefore serve as model for the putative arrangement of $[Ca(C_{52}H_{60}O_{12})]^{2-}$ moieties at the air-water interface at *low* surface pressure π.

Crystal structure of 3

Single crystals of the Ca complex **3** were obtained by slow re-crystallization of the crude product from MeOH/H_2O mixtures (10/1 vol.%) held at 90 °C. The Ca complex may be formally described as a coordination polymer with the sum formula 1/n $[Ca(C_{52}H_{60}O_{12})Ca(H_2O)_{2.5}(MeOH)_{0.5}]_n \cdot 7H_2O \cdot CH_3OH$ ($C_{53.5}H_{85}O_{23}Ca_2$, **3**).

Apparently, a 1:1 complex of a single Ca ion and the octadentate ligand **1** forms at the beginning, which possesses a two-fold net negative charge under the chosen reaction conditions (excess of $Ca(OH)_2$). The non-coordinated carboxylic acid oxygen donors of each mononuclear $[Ca(C_{52}H_{60}O_{12})]^{2-}$ building block can then bind to excess "free" calcium ions in solution to build up a coordination polymer.

The coordination environments of Ca ions in the crystal structure of **3** are quite different: The Ca ion (Ca(1), Fig. 4) sequestered by the calix[4]arene ligand **1** is eight-fold coordinated. As in the crystal structure of **2**, the Ca(1) coordination polyhedron may be described as an intermediate form between a square antiprism and a cube. The square planes spanned by the phenolic and the carboxylate oxygen donors, respectively, are rotated by 34° against each other. In contrast, the bridging metal ions (Ca(2)) are in a distorted pentagonal-bipyramidal coordination environment; each Ca ion is coordinated by four oxygen donors of three different calix[4]arene ligands and the coordination number is completed by two water ligands and a further oxygen donor of a monodentate MeOH ligand. The Ca(2) ions form doubly bridged, dinuclear units with a short Ca···Ca distance of 3.98(1) Å (Fig. 5). Each $[Ca(C_{52}H_{60}O_{12})]^{2-}$ building block is coordinated to three different Ca ions (μ_3-bridging mode).

Due to the stoichiometric (2:1) ratio of Ca ions and (deprotonated) calix[4]arene ligands, electrostatically neutral, one-dimensional coordination polymers form which have a dumb-bell shape in cross-sectional view. The coordination strands run in the *c* direction of the crystal lattice (Fig. 6). There are no coordinative bonds between coordination strands next to each other, which may explain the solubility of the complex in trichloromethane. The voids in the packing of coordination strands are filled with (non-coordinated) H_2O/MeOH molecules. In analogy to the lamellar arrangement of the calix[4]arene moieties in the crystal structure of **2**, compound **3** forms a bilayer structure where the polar functional groups and the hydrophobic residues segregate into different layers. Each bilayer runs parallel to the *bc* crystal plane while distinct bilayers are stacked along

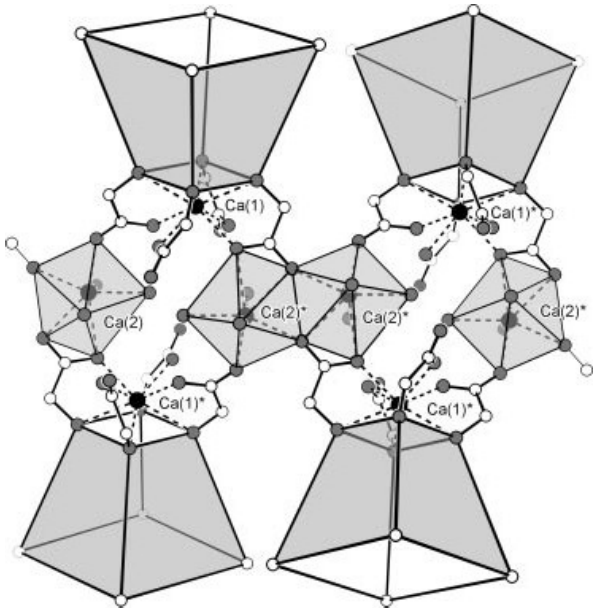

Fig. 4 Simplified representation of the coordination scheme of **3** (coordination polyhedrons are displayed for interconnecting Ca ions only). Selected Ca···Ca non-bonding distances:

Ca(1)···Ca(2): 5.98(1), Ca(1)···Ca(2)*: 4.58(1), Ca(2)···Ca(2)*: 3.98(1), Ca(2)···Ca(2)*: 6.92(1) Å.

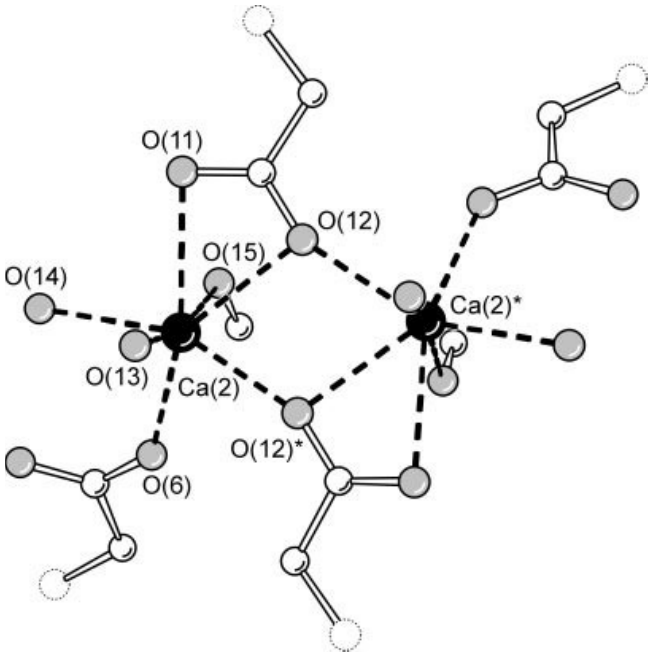

Fig. 5 Ball-and-stick model of the dinuclear Ca centers in the crystal structure of **3**.
(The carboxylate groups shown here are part of different calix[4]arene ligands (**1**), most atoms of which are omitted for clarity). Selected Ca−O bond lengths:

Ca(2)−O(6): 2.31(1) Ca(2)−O(11): 2.57(1), Ca(2)−O(12): 2.50(1), Ca(2)−O(13): 2.35(1), Ca(2)−O(14): 2.34(1), Ca(2)−O(15): 2.35(1), Ca(2)−O(12)*: 2.35(1) Å.

the *a* direction. Within the layer, calix[4]arene molecules are close packed with their pseudo C_{4v} symmetry axis tilted by 18° against the *bc*-plane normal. The average surface area occupied by a single calix[4]arene molecule in **3** amounts to 1.33 nm^2 which is considerably lower than the corresponding value calculated from the crystal structure of **2** (Table 2).

A further examination of the arrangement of calix[4]arene ligands in the crystal structure of **3** shows that the packing density of the hydrophobic residues should be close to the maximum reachable value since each *t*-butyl substituent of the ligand is at a van-der-Waals distance to its neighbours. The packing of calix[4]arene ligands in the *bc*-plane of **3** may therefore serve as model for the putative arrangement of $[Ca(C_{52}H_{60}O_{12})]^{2-}$ moieties at the air-water interface at *high* surface pressure π. (Packing plots for the in-plane arrangement of calix[4]arene ligands in the crystal structures of **2** and **3**, respectively, are provided as supplementary material).

Monolayer studies

Crystallographic investigations on the solid state structures of Ca salts of **1** are complemented by monolayer studies. Langmuir monolayers were formed on aqueous subphases by spreading compound **1** from trichloromethane solution using a Langmuir trough. The surface pressure−area (π−A) isotherms provide information on monolayer stability and phase behaviour. Fig. 7 shows the π−A isotherms of compound **1** monolayers spread on an aqueous subphase (Millipore water, or $CaCl_2/NaHCO_3$ (c = 9/18 mM), respectively).

In both cases, relatively stable monolayers form which collapse upon compression at a surface pressure of

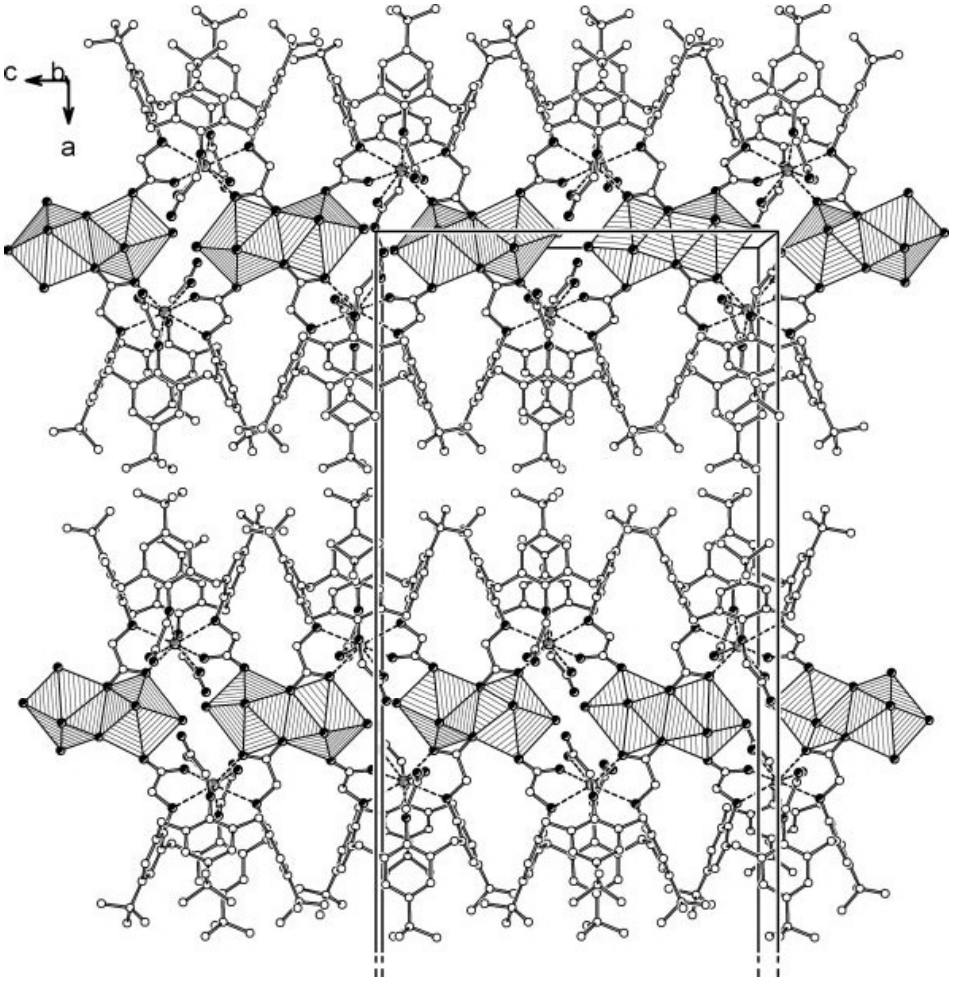

Fig. 6 Ball-and-stick model of the coordination polymer **3** showing the packing arrangement of the one-dimensional polymeric strands in the crystal lattice. (Solvent molecules occluded in the crystal lattice and hydrogen atoms are omitted for clarity. Coordination polyhedrons are displayed for interconnecting Ca ions only.)

Table 2 Area/molecule of calix[4]arene tetraacid derivatives as determined from Langmuir isotherms and from crystal data

Compound	Area/molecule/nm^2		Inclination angle/° [c]	Ref.
	Monolayer (subphase)	Crystal data (compound)		
1	1.15−1.20 (H_2O)[a]	n.d.	n.d.	this work
	1.30−1.40 ($Ca(HCO_3)_2$)[b]	1.70 (**2**)	25, 18[d]	this work
		1.33 (**3**)	18	this work
4	1.45−1.50 (H_2O)[a]	1.51 (**5**)	24	[7]
	1.70−1.75 ($Ca(HCO_3)_2$)[b]	1.70 (**6**)	34, 24[d]	[21]

Compound index: **1**: $C_{52}H_{64}O_{12}$, **2**: $[(Ca(C_{52}H_{60}O_{12}))_2Ca(H_2O)_2(CH_3OH)_3Ca(H_2O)_2(CH_3OH)_2]\cdot 12CH_3OH\cdot 4H_2O$, **3**: $[Ca(C_{52}H_{60}O_{12})Ca(H_2O)_{2.5}(MeOH)_{0.5}]\cdot 7H_2O\cdot CH_3OH$, **4**: $C_{68}H_{96}O_{12}$, **5**: $C_{68}H_{96}O_{12}\cdot 4.75CH_3OH\cdot 0.25H_2O$, **6**: $[Ca(C_{68}H_{92}O_{12}Ca)(DMSO)_2(H_2O)]\cdot 2.5DMSO$
n.d. = not determined
[a] Millipore water, resistance 18.2 MΩ·cm)
[b] Aqueous subphase containing $CaCl_2/NaHCO_3$, c = 9/18 mM
[c] Angle between the pseudo C_{4v} symmetry axis of the calix[4]arene molecule and the plane normal of the most densely packed crystal plane
[d] Two symmetry-independent calixarene molecules/asymmetric unit

~30 mN/m (pure water) and ~40 mN/m (Ca containing aqueous subphase), respectively. The featureless isotherms suggest fluid properties of the condensed phase in both cases. On water the onset of pressure increase is at ~1.30 nm^2/molecule whereas the surface pressure of the Ca containing solution starts to rise at a significantly higher value (~1.80 nm^2/molecule). We assume that this behaviour is due to electrostatic/coordinative interactions of Ca ions which cause the carboxylic acid residues of **1** to become deprotonated. Expansion effects of monolayers spread on metal ion-containing subphases, similar to those observed here, have been reported for several systems [11].

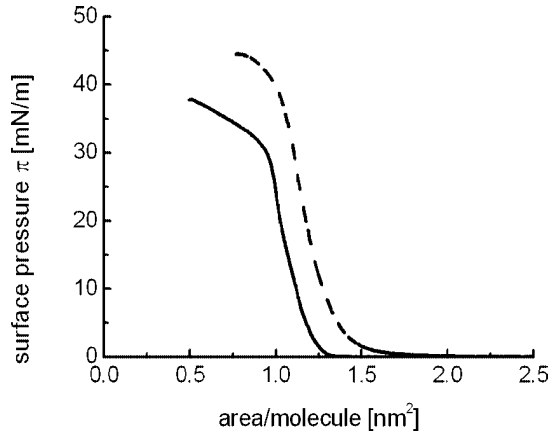

Fig. 7 π-A isotherms of monolayers of **1** at 22 °C on H_2O (solid line), and aqueous $CaCl_2/NaHCO_3$ (c = 9/18 mM, dashed line).

The area per molecule of **1** in the monolayers is estimated from extrapolating the Langmuir isotherms toward zero pressure. The determined area values are listed in Table 2. Monolayer data are in excellent agreement with the surface areas per molecule as determined from crystal structure analysis. The monolayer data show that the packing density of ligand **1** in the monolayer and in the crystal lattices of **2** and **3** are similar. The two-dimensional packing arrangement of **1** in the monolayer at low surface pressure (π ~ 0.5 mN/m) is presumably determined by the (highly solvated) polar carboxylate residues and the diffuse layer of Ca ions underneath the monolayer. The packing density of **1** in the crystal structure of compound **2** is almost identical to the corresponding value of the monolayer (~1.80 nm^2/molecule) at the beginning of compression. We, therefore, suggest that *at low surface pressure* the monolayer mainly consists of oligomeric Ca complexes of **1** which rapidly form. These complexes are free-floating at the air−water interface and they can easily rearrange their relative positions in order to adapt to the rising surface pressure. Upon further compression the complexes start to approach each other until the critical van-der-Waals distance to their nearest neighbours is reached. The crystal structure of compound **3** in fact shows that a highly symmetrical, planar, close-packed arrangement of the hydrophobic *t*-butyl groups is feasible, although intuitively one may assume that the conical shape of the calix[4]arene ligand should introduce some curvature in the layer structure. However, the fact that the C_{4v} symmetry axes of the calix[4]arene units in the crystal structure of **3** are tilted by 18° against the plane normal gives us a hint that the packing affords a compromise between the most *symmetrical* and the most *dense* arrangement of conically shaped amphiphiles. Interestingly, the av. area/molecule of 1.33 nm^2 as calculated from the crystal data of compound **3** corresponds to a surface pressure value of ~6 mN/m in the monolayer. Assuming a similar arrangement of calix[4]arene ligands in the crystal structure and the monolayer, this would mean that a relatively high and constant, external pressure is required in order to force the calix[4]arene units into this periodic arrangement. It should be noted that crystals of compound **3** in fact were grown under "hydrothermal" conditions, i.e. the solution was kept within firmly sealed test tubes and the re-crystallization temperature was allowed to exceed the boiling point of the solvent mixture.

We would like to stress the point that neither the isotherms of **1** monolayers on pure water nor on a Ca containing subphase indicate the formation of a liquid crystalline phase. While the local arrangement of calix[4]arene moieties in the monolayer and crystal structure might be similar, the monolayer phase clearly lacks the long range order of the crystalline material.

However, it is a common observation that crystalline monolayers composed of molecules which are structurally more complex than the most simple amphiphiles (e.g. monofunctional surfactants with a single saturated hydrocarbon chain) are hardly obtained. A possible reason for this might be that, in the present and related cases, the time frame for recording the Langmuir isotherms is insufficient in order to allow nucleation/growth of two-dimensional crystalline patches to proceed in the compressed monolayer.

$CaCO_3$ crystallization underneath monolayers

Crystallization of calcium carbonate underneath monolayers of **1** leads to formation of uniformly oriented calcite

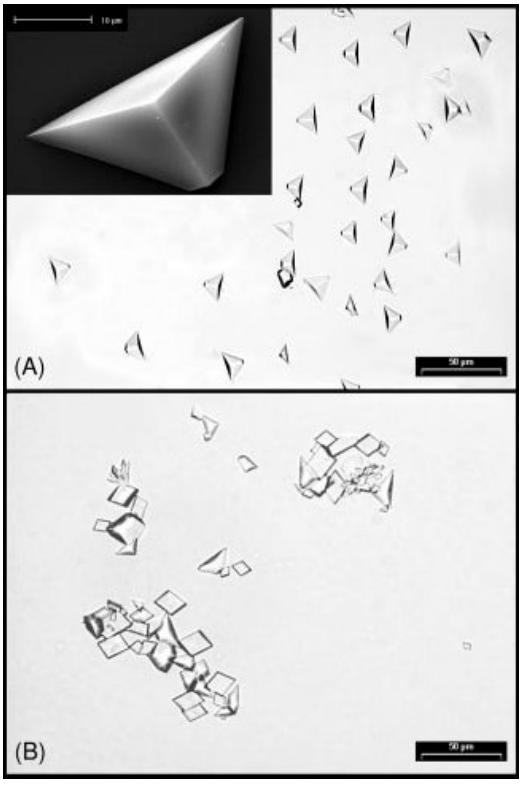

Fig. 8 Optical micrographs of calcite single crystals grown under a monolayer of 1 after 4 h. (**A**) π = 0.1 mN/m, $CaCl_2/NaHCO_3$ (c = 9/18 mM). The inset shows a scanning electron micrograph of a (012) oriented calcite single crystal grown under the same conditions. (**B**) π = 6 mN/m, $CaCl_2/NaHCO_3$ (c = 9/18 mM).

single crystals at low surface pressure ($\pi = 0.1 - 0.5$ mN/m) and a molecular area of $1.70 - 1.80$ nm^2. At a higher surface pressure ($\pi = 5 - 12$ mN/m) and a molecular area of $1.25 - 1.35$ nm^2 the calcite crystals grown underneath the monolayer lack any preferential orientation. Due to insufficient long-term stability of the monolayer at a surface pressure exceeding 20 mN/m, crystallization experiments under these conditions were impracticable.

Crystal growth was observed *in situ* by optical microscopy (Fig. 8). The orientation of calcite crystals was determined by X-ray powder diffraction and geometrical analysis. A more detailed description of the procedure is given elsewhere [7].

The calcite single crystals obtained at low surface pressure display the typical shape of truncated rhombohedrons (Fig. 8A and inset). The truncation occurs parallel to the {01.2} faces of the calcite crystal lattice [4, 12]. In contrast, the crystals which grow underneath the monolayer of **1** at a high surface pressure often possess the highly symmetrical shape of the calcite {10.4} cleavage rhombohedron (Fig. 8B). The nucleation density at high surface pressure is reduced (approximately 1/5) and the spacing between different calcite crystals attached to the monolayer is much less regular as compared to low surface pressure conditions. These observations indicate that at low surface pressure ($\pi = 0.1 - 0.5$ mN/m), the monolayer directs nucleation and growth of the calcite crystals while at higher surface pressure ($\pi = 5 - 12$ mN/m) crystal growth becomes inhibited [18].

Crystallization of (012) oriented calcite crystals has been reported for other self-assembled systems as well. These include polymeric Langmuir-Schaefer films of 10,12-pentacosadiynoic acid, [3d, 13] self-assembled monolayers of carboxylate-terminated alkanethiols supported on silver [4, 14] or Au substrates, [15] as well as hydrogen-bonded molecular ribbons consisting of N,N′-dioctadecyltriazine-2,4,6-triamine and a cyanuric acid derivative [3f]. The templating role of the monolayer has been interpreted in terms of geometrical lattice matching and stereochemical complementarity between the monolayer head groups and the (01.2) crystal plane attached to the monolayer.

We, too, have observed preferential crystallization of (01.2) oriented calcite crystals underneath a variety of structurally dissimilar monolayers. While in all of our investigations we have consistently employed monolayers of tetradentate amphiphilic macrocycles, the molecular structures of the compounds and their crystal packing arrangements differed significantly. Thus, monolayers of amphiphilic calix[4]arene derivatives which possess hydrophobic substituents of varying steric demands [7, this study] as well as amphiphilic resorc[4]arene derivatives (e.g. *rccc*-5,11,17,23-tetracarboxy-4,6,10,12,16,18,22,24-octa-*O*-methyl-2,8,14,20-tetra-(n-undecyl)resorc[4]arene, [16] which are structurally complementary to calix[4]arene ligands, uniformly led to the same orientation of calcite crystals. Since furthermore, the oriented growth of calcite single crystals underneath the monolayers always and exclusively occurred at very low surface pressure, where the monolayers exist in a liquid-expanded state, an epitaxial correlation of the monolayer "lattice" and the {01.2} crystal plane might in fact be ruled out. Our experiments indicate that a low surface pressure is a necessary condition for the growth of uniformly oriented calcite crystals. Under these conditions the amphiphilic molecules in the monolayer may freely rearrange in order to minimize the lattice mismatch with the nucleating crystal face, thereby reducing the interfacial tension of the system [17]. We suggest that non-specific electrostatic effects such as the average charge density or the mean dipole moment of the monolayer determine the orientation of crystals [7, 18]. In fact in all of our investigations, the growth of (01.2) oriented calcite crystals occurred at a surface area corresponding to $1.70 - 1.80$ nm^2/molecule which leads to an av. density of $2.22 - 2.35$ carboxylate residues/nm^2. This hypothesis is further supported by our recent investigations [19] on calcium carbonate growth underneath monolayers of *rccc*-4,6,10,12,16,18,22,24-octa-*O*-(carboxymethyl)-2,8,14,20-tetra-(n-undecyl)resorc[4]arene, where a change in the number of coordinating residues per molecule (8 instead of 4) leads to a completely different calcium carbonate growth characteristics (*vide infra*). Efforts are currently undertaken to analyze the particular growth orientation of calcium carbonate crystals in this and likewise systems.

Experimental Section

Melting points were determined with a Electrothermal melting point apparatus and were uncorrected. FT-IR spectra were recorded from KBr pellets on a Shimadzu FTIR-8300 spectrometer. ^{1}H and ^{13}C NMR spectra were recorded on a Bruker DRX 500 spectrometer in DMSO-d_6 at room temperature with residual solvent.

Mass spectra were recorded with a Micromass VG Autospec X, Voyager DE spectrometer. Elemental analysis were carried out with a Perkin-Elmer 240 elemental analyzer. All reagents were reagent grade and used without further purification.

5,11,17,23-tetra-*t*-butyl-25,26,27,28-tetrakis-(carboxymethoxy)calix[4]arene (1):

The product was prepared according to a slightly modified literature procedure [20]. To a solution of 5,11,17,23-tetra-*t*-butyl-25,26,27,28-tetrakis(ethoxycarbonylmethoxy) calix[4]arene (0.495 g, 0.5 mmol) in tetrahydrofurane (30 mL) was added an aqueous solution of tetramethylammonium hydroxide (25 %, 12.8 mL, 35.4 mmol) and the suspension was heated under reflux. After 24 h the suspension was concentrated under reduced pressure, the residue was dissolved in chloroform (20 mL), rinsed with hydrochloric acid (2 × 20 mL) and water (5 × 20 mL). The organic layer was concentrated *in vacuo* and the crude product was re-crystallized from acetonitrile (3 × 100 mL) to give the final product in 70 % yield: m.p. 270-272 °C (CH_3CN);

IR (cm^{-1}): $\tilde{\nu}$ = 3412, 2961, 1735, 1480, 1242, 1192, 1129, 1057, 870.
^{1}H NMR (DMSO-d_6, 500 MHz) δ = 6.94 (s, 8H, ArH), 4.76 (d, 4 H ($ArCH_2$), 4.58 (s, 8 H, CH_2COO), 3.22 (d, 4 H, $ArCH_2$), 1.55 (s, 3 H, CH_3CN), 1.05 (s, 36 H, CH_3).

^{13}C-NMR (125 MHz) δ = 171.00 (CH_2COO), 152.36 (ArCO), 145.27 (ArC*t*Bu), 133.45 (ArCH), 125.41 (ArCCH_2), 118.08 (CH_3CN), 71.77 (OCH_2), 33.70 (CH_2Ar), 31.22 ($C(CH_3)_3$), 30.85 ($C(CH_3)_3$).

MALDI-MS (matrix 2,5-dihydroxybenzoic acid): *m/z* = 904 [M$^+$ + Na, 100 %]; **Elemental analysis** calc. for $C_{52}H_{64}O_{12} \cdot CH_3CN$: C 69.95, H 7.42, N 1.54; found: C 69.93, H 7.18, N 1.54 %.

$[(Ca(C_{52}H_{60}O_{12}))_2Ca(H_2O)_2(CH_3OH)_3Ca(H_2O)_2\text{-}(CH_3OH)_2]\cdot 12CH_3OH\cdot 4H_2O$ (2)

5,11,17,23-tetra-*t*-butyl-25,26,27,28-tetrakis(carboxymethoxy)-calix[4]arene (44 mg, 0.05 mmol) and calcium hydroxide (11 mg, 0.15 mmol) were suspended in MeOH abs. (30 mL). The suspension was treated ultrasonically and filtered into a 6 well NUNC multidish with 6 wells. Into each well H_2O (200 µL) was introduced, the wells were covered with parafilm, and the parafilm was punctured by a needle. The multidish was placed in a sealed desiccator containing a beaker filled with H_2O. Single crystals of **2** grew within a period of 24h.

$[Ca(C_{52}H_{60}O_{12})Ca(H_2O)_{2.5}(MeOH)_{0.5}]_n\cdot 7H_2O\cdot CH_3OH$ (3)

5,11,17,23-tetra-*t*-butyl-25,26,27,28-tetrakis(carboxymethoxy)-calix[4]arene (44 mg, 0.05 mmol) and calcium hydroxide (11 mg, 0.15 mmol) were suspended in H_2O (10 mL). The suspension was treated ultrasonically and centrifuged. The pellet was suspended in H_2O (10 mL), treated ultrasonically and was centrifuged. The wet residue was dissolved in MeOH abs. (6 mL) and crystallized at 90 °C. Colourless crystals were obtained after 5 days.
IR (cm^{-1}): $\tilde{\nu}$ 3414, 2959, 1616, 1475, 1425, 1333, 1242, 1192, 1126, 1018, 943, 872, 829.
(IR spectra of **2** and **3** are virtually indistinguishable).

X-Ray Structure Analysis

Details of structure refinement and X-ray crystallographic data are provided as supplementary information. Crystallographic data (excluding structure factors) for the structure reported in this paper have been deposited at the Cambridge Crystallographic Data Centre as supplementary publication CCDC no. 216527 (compound **2**) and CCDC no. 216528, (compound **3**), respectively. Copies of the data can be obtained free of charge on application to CCDC, 12 Union Road, Cambridge CB21EZ (Fax:(+44)1223-336-033; e-mail: deposit@ccdc.cam.ac.uk).

Monolayer Investigations

Monolayer experiments were performed with a double-barrier NIMA trough using a compression speed of 15 cm^2/min. The surface pressure of the monolayers was measured using a Wilhelmy plate. The surfactant was spread using a chloroform solution (10 µl, 0.5 mg/mL). Compression was started after 10 min.

$CaCO_3$ Crystal Growth Experiments

Solutions of calcium bicarbonate were prepared by bubbling carbon dioxide gas through a stirred aqueous (Millipore water, resistance 18.2 MΩ·cm) solution of $CaCl_2$/$NaHCO_3$ (c = 9/18 mM) for a period of 2 h. Compressed films were formed by adding known amounts of surfactant to generate a liquid- or solid-like film at the air-water interface. Crystals were studied after several times either *in situ* by optical microscopy (Olympus IX 70) or on cover slips laid on the film. The cover slips were also mounted on scanning electron microscope (SEM) specimen tubs. A Phillips XL30 ESEM operating at 30 keV was used. The calcite crystals were sputtered with Au prior to examination.
Bulk samples for X-ray diffraction (XRD) were obtained by collecting the crystals on cover slips laid on the film and removed horizontally. A Philips PW 1050/70 X-ray powder diffractometer was employed (2θ scans, Bragg-Brentano para-focussing geometry) using CuK_α radiation (λ = 1.54 Å).
Crystallographic indices are presented in three-index (*hkl*) notation, based on the hexagonal setting of the calcite unit cell ($R\bar{3}c$, *a* = 4.96 Å, *c* = 17.002 Å).

Acknowledgements. D.V. thanks the DFG for a Habilitanden fellowship. M.F. thanks the Graduiertenförderung Nordrhein-Westfalen for a graduate fellowship. This work was financially supported by the Deutsche Forschungsgemeinschaft (DFG Schwerpunktprogramm 1117, "Prinzipien der Biomineralisation"; DFG grant Vo829/2-1).

References

[1] a) H. A. Lowenstam, S. Weiner, *On Biomineralization*, Oxford University Press, Oxford **1989**; b) S. Mann, *Biomineralization. Principles and Concepts in Bioinorganic Materials Chemistry*, Oxford University Press, Oxford, **2001**; c) L. Addadi, S. Weiner, *Angew. Chem., Int. Ed. Engl.* **1992**, *31*, 153–169; d) L. Addadi, S. Weiner, *Proc. Natl. Acad. Sci. U.S.A.* **1985**, *82*, 4110–4114; e) S. Weiner, L. Addadi, *J. Mater. Chem.* **1997**, *7*, 689–702; f) A. M. Belcher, X. H. Wu, R. J. Christensen, P. K. Hansma, G. D. Stucky, D. E. Morse, *Nature* **1996**, *381*, 56–58.
[2] a) S. Mann, *Biomimetic Materials Chemistry*, VCH, Weinheim **1996**; b) H. Rapaport, I. Kuzmenko, M. Berfeld, K. Kjaer, J. Als-Nielsen, R. Popovitz-Biro, I. Weissbuch, M. Lahav, L. Leiserowitz, *J. Phys. Chem. B* **2000**, *104*, 1399–1424; c) S. Mann, D. D. Archibald, J. M. Didymus, T. Douglas, B. R. Heywood, F. C. Meldrum, N. J. Reeves, *Science* **1993**, *261*, 1286–1292; d) B. R. Heywood, S. Mann, *Adv. Mater.* **1994**, *6*, 9–20; e) E. Dujardin, S. Mann, *Adv. Mater.* **2002**, *14*, 775–788.
[3] a) S. Mann, B. R. Heywood, S. Rajam, J. D. Birchall, *Nature* **1988**, *334*, 692–695; b) S. Rajam, B. R. Heywood, J. B. A. Walker, S. Mann, R. J. Davey, J. D. Birchall, *J. Chem. Soc., Faraday Trans.* **1991**, *87*, 727–734; c) B. R. Heywood, S. Mann., *Chem. Mater.* **1994**, *6*, 311–318; d) A. Berman, D. J. Ahn, A. Lio, M. Salmeron, A. Reichert, D. Charych, *Science* **1995**, *269*, 515–518; e) G. Xu, N. Yao, I. A. Aksay, J. T. Groves, *J. Am. Chem. Soc.* **1998**, *120*, 11977–11985; f) S. Champ, J. A. Dickinson, P. S. Fallon, B. R. Heywood, M. Mascal, *Angew. Chem. Int. Ed. Engl.* **2000**, *39*, 2716–2719; g) P. J. J. A. Buijnsters, J. J. J. M. Donners, S. J. Hill, B. R. Heywood, R. J. M. Nolte, B. Zwanenburg, N. A. J. M. Sommerdijk, *Langmuir* **2001**, *17*, 3623–3628; h) E. DiMasi, V. M. Patel, M. Sivakumar, M. J. Oltsza, Y. P. Yang, L. Gower, *Langmuir* **2002**, *18*, 8902–8909.
[4] a) J. Aizenberg, A. J. Black, G. M. Whitesides, *J. Am. Chem. Soc.* **1999**, *121*, 4500–4509; b) J. Küther, G. Nelles, R. Seshadri, M. Schaub, H. J. Butt, W. Tremel, *Chem. Eur. J.* **1998**, *4*, 1834–1842; c) D. D. Archibald, S. B. Qadri, B. P. Gaber, *Langmuir* **1996**, *12*, 538–546.
[5] a) L. Addadi, J. Moradian, E. Shay, N. G. Maroudas, S. Weiner, *Proc. Natl. Acad. Sci. U.S.A.* **1987**, *84*, 2732–2736; b)

S. R. Letellier, M. J. Lochhead, A. A. Campbell, V. Vogel, *Biochim. Biophys. Acta* **1998**, *1380*, 31–45.
[6] L. Addadi, S. Weiner, in: *Biomineralization*, S. Mann (ed), VCH, Weinheim **1989**, pp. 133–156.
[7] D. Volkmer, M. Fricke, D. Vollhardt, S. Siegel, *J. Chem. Soc., Dalton Trans.* **2002**, 4547–4554.
[8] D. Volkmer in *Encyclopedia of Separation Science*, M. Cooke, C.F. Poole (eds.), Vol. 2 (Crystallization), Academic Press **2000**, pp. 940–950.
[9] P.M. Harrison, P. Arosio, *Biochim. Biophys. Acta* **1996**, *1275*, 161–203.
[10] H. Ti Tien, in: *Thin Liquid Films*, I. B. Ivanov (ed), *Surfactant Science Series*, Vol. 29, **1988**, pp. 927–1057.
[11] a) V. A. Arsentiev and J. Leja, in: *Colloid and Interface Science*, M. Kerker, (ed), Vol. 5, Academic Press, New York **1976**, pp. 251–270; b) G.T. Barnes, in: *Colloid Science*, D.H. Everett (ed), Vol. 2, Chemical Society, London 1975, pp. 173–190.
[12] S. J. Cooper, R. B. Sessions, S. D. Lubetkin, *J. Am. Chem. Soc.* **1998**, *120*, 2090–2098.
[13] J. Ahn, A. Berman, D. Charych, *J. Phys. Chem.* **1996**, *100*, 12455–12461.
[14] J. Aizenberg, Y-J. Han, *J. Am. Chem. Soc.* **2003**, *125*, 4032–4033.
[15] A. M. Travaille, J. J. J. M. Donners, J. W. Gerritsen, N. A. J. M. Sommerdijk, R. J. M. Nolte, H. van Kempen, *Adv. Mater.* **2002**, *14*, 492–495.
[16] D. Volkmer, M. Fricke, C. Agena, J. Mattay, *Cryst. Eng. Commun.* **2002**, *4*, 288–295.
[17] S. J. Cooper, R. B. Sessions, S. D. Lubetkin, *Langmuir* **1997**, *13*, 7165–7172.
[18] a) M. J. Lochhead, S. R. Letellier, V. Vogel, *J. Phys. Chem.* B **1997**, *101*, 10821–10827; b) P. Calvert, S. Mann, *Nature* **1997**, *386*, 127–129.
[19] D. Volkmer, M. Fricke, unpublished results.
[20] S.-K. Chang, I. Cho, *J. Chem. Soc., Perkin Trans.* I **1986**, 211–214.
[21] D. Volkmer, M. Fricke, unpublished results.